Supporting Information

Mocibob et al. 10.1073/pnas.1007470107

SI Text

SI Materials and Methods. ***Gene cloning, protein overexpression, and purification.*** Genes for aSerRS homologs (Atu2573, Bll0957, and Bll6282), putative carrier proteins (CPs) (Atu2571, Bsr0959, and Blr6284) and acyl CPs (from *Agrobacterium tumefaciens, Bradyrhizobium japonicum*, and *Escherichia coli*) were amplified by PCR from genomic DNA and cloned into pET28b (Novagen) in NdeI and XhoI or NdeI and BamHI restriction sites, in frame with N-terminal His-tag coding sequence. Proteins were overexpressed in *E. coli* BL21(DE3) at 30 °C after induction with 1 mM IPTG and purified by affinity chromatography on Ni-NTA agarose (Qiagen) by standard procedures. Carrier protein Blr6284 was purified from inclusion bodies, after solubilization with 8 M urea under denaturing conditions on Ni-NTA agarose. Blr6284 was refolded by 200-fold dilution in buffer without urea.

Genes for fusion proteins of mMbSerRS N-terminal domain (residues 1–167) and aSerRS homologs were constructed by overlap PCR (1) using pET28 constructs and pET15mMbSerRS (2) as templates. PCR fragments were cloned to pET28b, and N-terminal His-tagged fusion proteins were overexpressed and purified as described.

Phosphopantetheinylation of CPs. Purified apo-forms of vicinal CPs and acyl CPs (ACPs) were phosphopantetheinylated enzymatically, using the promiscuous 4′-phosphopantetheinyl transferase Sfp from *Bacillus subtilis*. ApoCPs (1 mg/mL) were incubated with Sfp (0.012–0.1 mg/mL), 0.5 mM coenzyme A (CoA), 10 mM $MgCl_2$ and 4 mM DTT for 45–60 min at room temperature. Buffer composition and pH was optimized for each CP. Reaction was terminated by CoA and Mg^{2+} removal by desalting on PD-10 columns. Samples were concentrated by ultrafiltration and further purified by size-exclusion chromatography on Superdex 75 10/300 GL column (GE Healthcare), to remove Sfp and traces of CoA and DTT. Modification of CPs was monitored by Tricine SDS-PAGE (3) and confirmed by mass spectrometry.

Isolation of unfractioned tRNA from A. tumefaciens and B. japonicum. *A. tumefaciens* and *B. japonicum* were grown in Luria-Bertani medium at 28 °C to late log phase. Nucleic acids were extracted from cell pellets by phenol extraction at 70 °C, essentially as previously described (4). High M_r nucleic acids (DNA, rRNA, and mRNA) were removed from crude extracts by PEG precipitation (10% (w/v) PEG 8000, 250 mM TrisHCl pH 8.8, 750 mM NaCl, 10 mM $MgCl_2$) at room temperature. Crude preparations of tRNA were deacylated and further purified by chromatography on DEAE-cellulose as previously described (4). Preparations of unfractioned tRNA from *A. tumefaciens* contained 4.6% $tRNA^{Ser}$ and 8.8% $tRNA^{Ala}$ isoacceptors, while *B. japonicum* bulk tRNA contained 5.4% $tRNA^{Ser}$ and 9.4% $tRNA^{Gly}$, as determined by aminoacylation with *E. coli* SerRS and *A. tumefaciens* or *B. japonicum* protein extracts. Unfractioned *E. coli* tRNA was purchased from Roche.

Data collection and structure refinement of Bll0957. A dataset of Bll0957 protein was collected at zinc peak wavelength of 1.282 Å at the synchrotron beamline PROXIMA I (Soleil, France). The crystal structure was determined using single-wavelength anomalous diffraction phasing. Data were indexed, integrated, and scaled with XDS (5), and phases were obtained using autoSHARP (6). ARP/wARP (7) was used for automated model building. The rest of the model was manually built using COOT (8) and refined with Refmac (9) and Buster-TNT (10). The complete datasets of Bll0957:ATP and Bll0957:GlyAMS complexes were collected on in-house Xcalibur Nova R diffractometer (Oxford Diffraction). Scaling, merging, and conversion of the intensities to structure factors were carried out using the CCP4 (11) programs Scala and Truncate. COOT was used to model substrates into the active site and Refmac and Buster-TNT for rigid body and restrained refinement. Data collection and refinement statistics are summarized in Table S2.

Fluorescent labeling and MS analysis of aminoacylated CPs. 1 mg/mL of apo- or holo-CPs was incubated with 0.1 mg/mL aa:CP ligase in 50 mM TrisHCl pH 7.5, 150 mM KCl, 10% glycerol, 10 mM $MgCl_2$, 4 mM ATP, 500 μM Gly or Ala, 1 μg/mL yeast inorganic pyrophosphatase (Roche) at room temperature for 30 min followed by treatment of samples with equal volume of 8 mM fluorescein-5-maleimide (dissolved in *N*,*N*-dimethylformamide) for 5 min. Reaction was quenched by addition of SDS-PAGE sample loading buffer (containing excess β-mercaptoethanol) and samples were subjected to SDS-PAGE on 15% polyacrylamide gels. Fluorescent bands were visualized on Typhoon Trio (GE Healthcare).

Samples for MS analysis were prepared in the same manner, without treatment with fluorescein-5-maleimide and SDS-PAGE sample loading buffer. Samples were submitted to MALDI-MS analysis in the Functional Genomics Center Zurich (Switzerland).

1. Sambrook J, Russel DW (2001) *Molecular Cloning: A Laboratory Manual*, 3rd ed. (Cold Spring Harbor Laboratory Press, New York) 13.1–13.62.
2. Korencic D, Polycarpo C, Weygand-Durasevic I, Söll D (2004) Differential modes of transfer RNA^{Ser} recognition in *Methanosarcina barkeri*. *J Biol Chem* 279:48780–48786.
3. Schägger H (2006) Tricine–SDS-PAGE. *Nat Protoc* 1:16–22.
4. Mocibob M, Weygand-Durasevic I (2008) The proximal region of a noncatalytic eukaryotic seryl-tRNA synthetase extension is required for protein stability in vitro and in vivo. *Arch Biochem Biophys* 470:129–138.
5. Kabsch W (1993) Automatic processing of rotation diffraction data from crystals of initially unknown symmetry and cell constants. *J Appl Crystallog* 26:795–800.
6. Vonrhein C, Blanc E, Roversi P, Bricogne G (2007) Automated structure solution with autoSHARP. *Methods Mol Biol* 364:215–30.
7. Langer G, Cohen SX, Lamzin VS, Perrakis A (2008) Automated macromolecular model building for X-ray crystallography using ARP/wARP version 7. *Nat Protoc* 3:1171–1179.
8. Emsley P, Cowtan K (2004) *COOT*: model-building tools for molecular graphics. *Acta Crystallogr D* 60:2126–2132.
9. Murshudov GN, Vagin AA, Dodson EE (1997) Refinement of macromolecular structures by the maximum-likelihood method. *Acta Crystallogr D* 54:240–255.
10. Blanc E, et al. (2004) Refinement of severely incomplete structures with maximum likelihood in BUSTER-TNT. *Acta Crystallogr D* 60:2210–2221.
11. Collaborative Computational Project, Number 4. (1994) The CCP4 suite: programs for protein crystallography. *Acta. Crystallogr. D* 50:760–763.

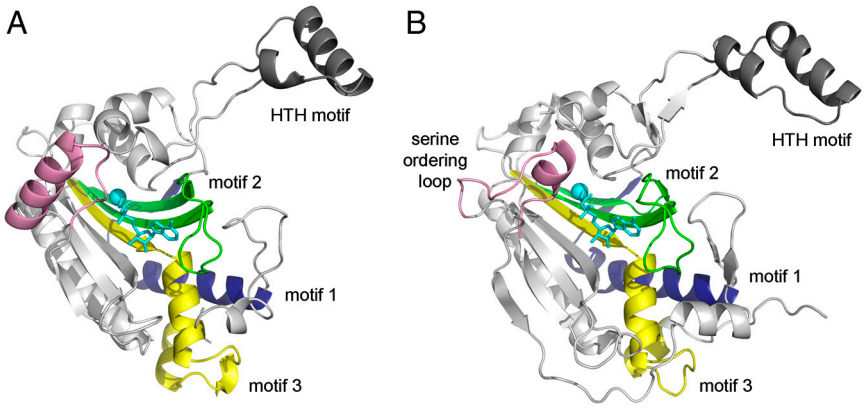

Fig. S1. Comparison of Bll0957 (*A*) and mMbSerRS catalytic domain (*B*). Three aaRS class II signature motifs 1, 2, and 3 are colored in blue, green, and yellow, respectively. Helix-turn-helix motifs idiosyncratic to aSerRS and their homologs are shown in darker shade of gray. Zinc atom and adenylate-analogs in the active site are shown in cyan. The "serine ordering loop" characteristic for mMbSerRS, and the corresponding helix in Bll0957, are colored pink.

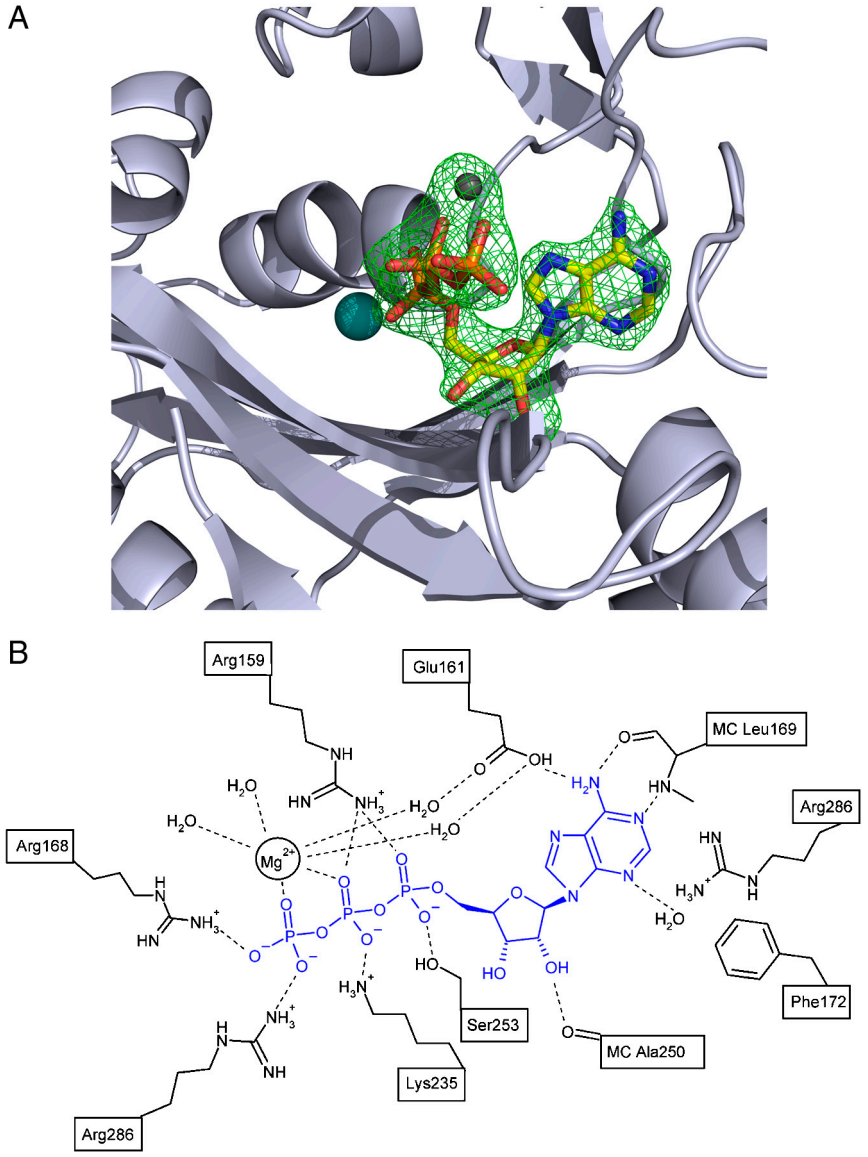

Fig. S2. The Bll0957:ATP complex. (*A*) Omit $F_o - F_c$ electron density map (resolution 2.5 Å, contour level 3.0σ) and the refined model. ATP and Mg^{2+} were omitted from the model during map calculation. Protein backbone is shown as a gray ribbon; zinc ion is in cyan and magnesium ion in dark gray. ATP is shown in ball-and-stick representation. (*B*) Schematic representation of the interactions between the enzyme, ATP, and magnesium.

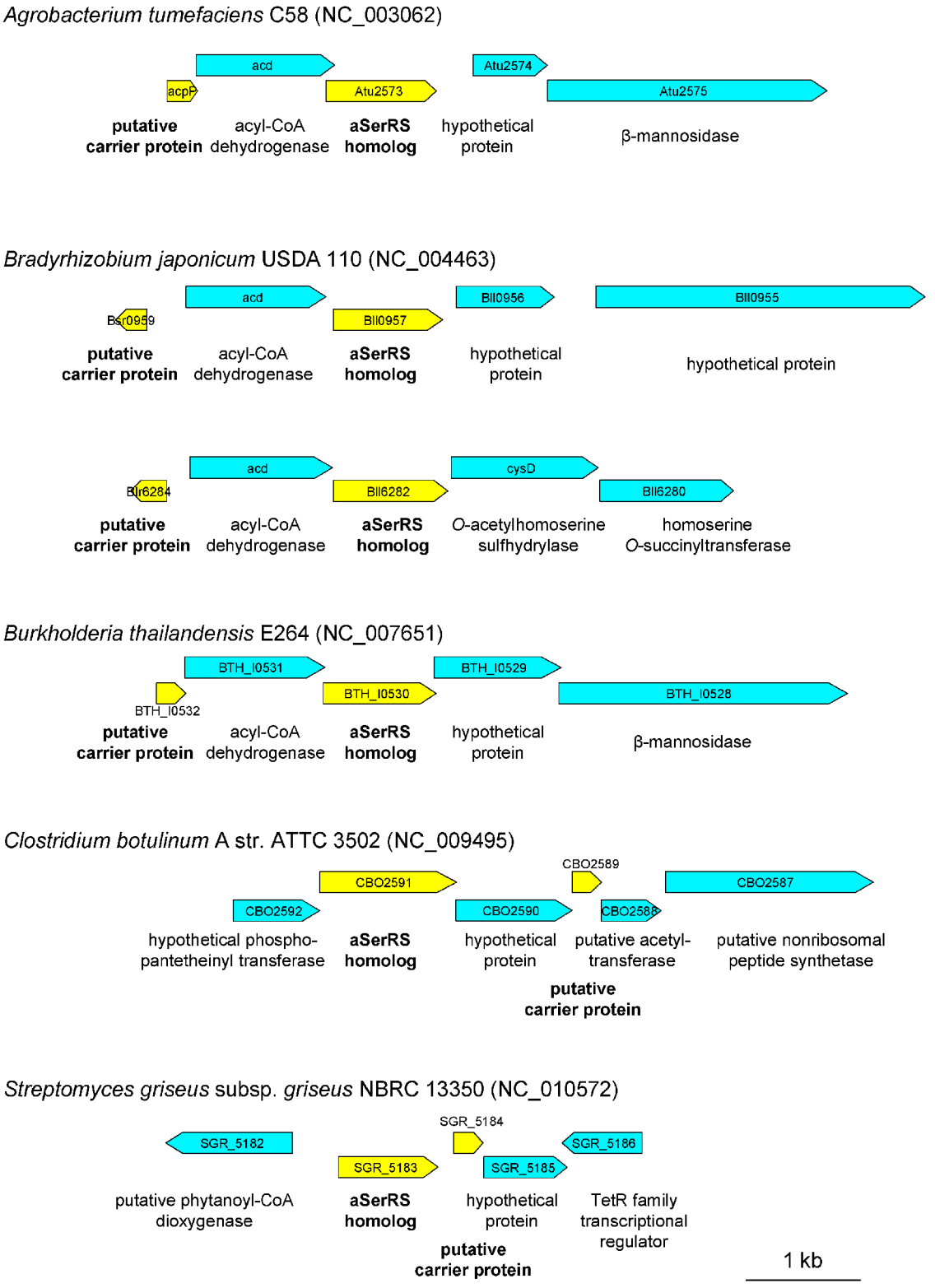

Fig. S3. Schematic representation of genomic surroundings of aSerRS homologs in the genomes of various representative bacteria. aSerRS homologs and accompanying putative CPs are highlighted. National Center for Biotechnology Information Nucleotide accession numbers of genomes analyzed are given in parenthesis.

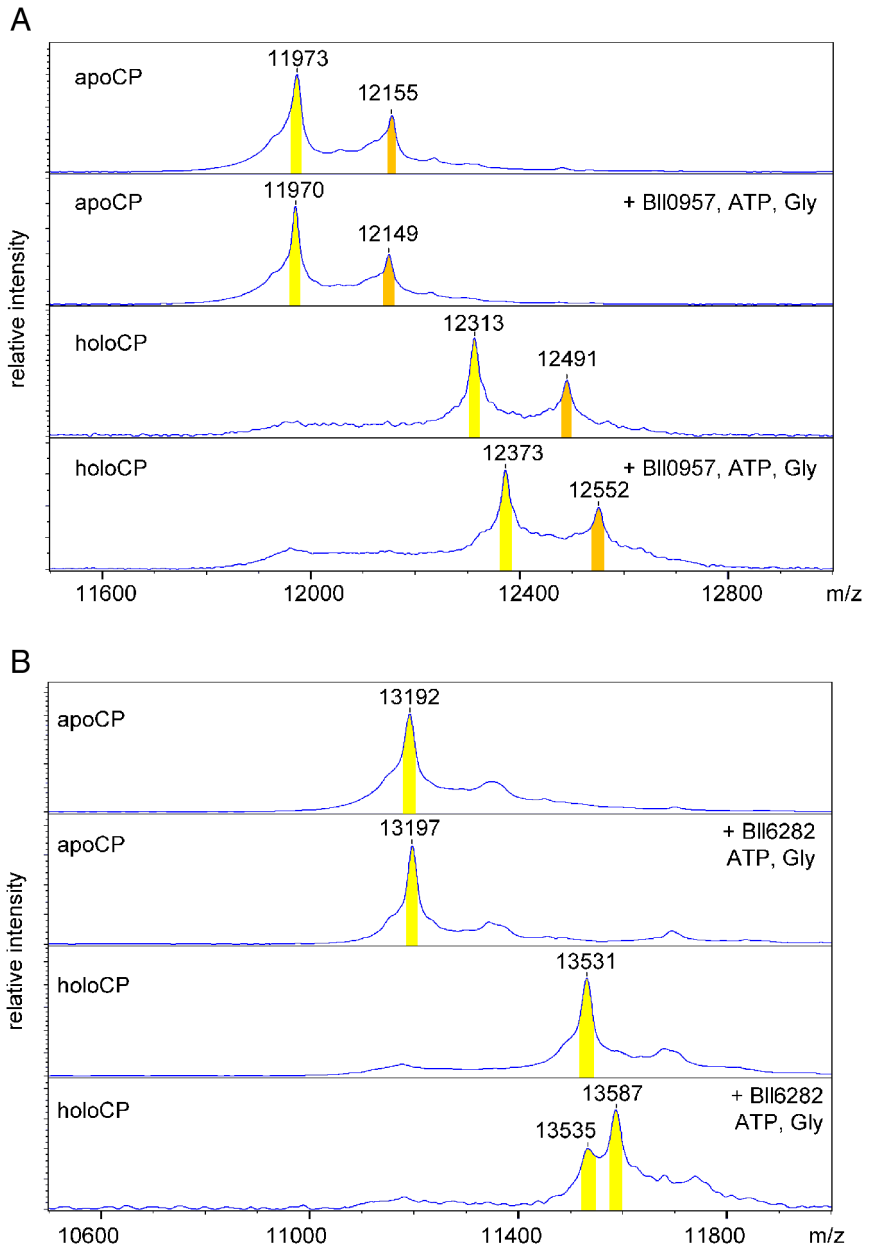

Fig. S4. MS analysis of CP aminoacylation by aSerRS homologs Bll0957 (*A*) and Bll6282 (*B*). Apo- and holoCP were incubated under identical conditions with or without addition of the enzymes (Bll0957 or Bll6282), ATP and amino acids. M_r difference ($\Delta M_r = 336–343$) between lanes 1 and 3 corresponds to M_r of phosphopantetheinyl prosthetic group (expected $M_r = 340$). M_r difference between lanes 3 and 4 ($\Delta M_r = 56–61$) matches M_r of glycyl- residue (expected $M_r = 58$). Preparation of CP cognate for Bll0957 (*A*) contains two different isoforms (yellow and orange peaks), $\Delta M_r = 180$, and both of them are phosphopantetheinylated by Sfp and acylated by Bll0957. These isoforms were consistently observed in different CP preparations.

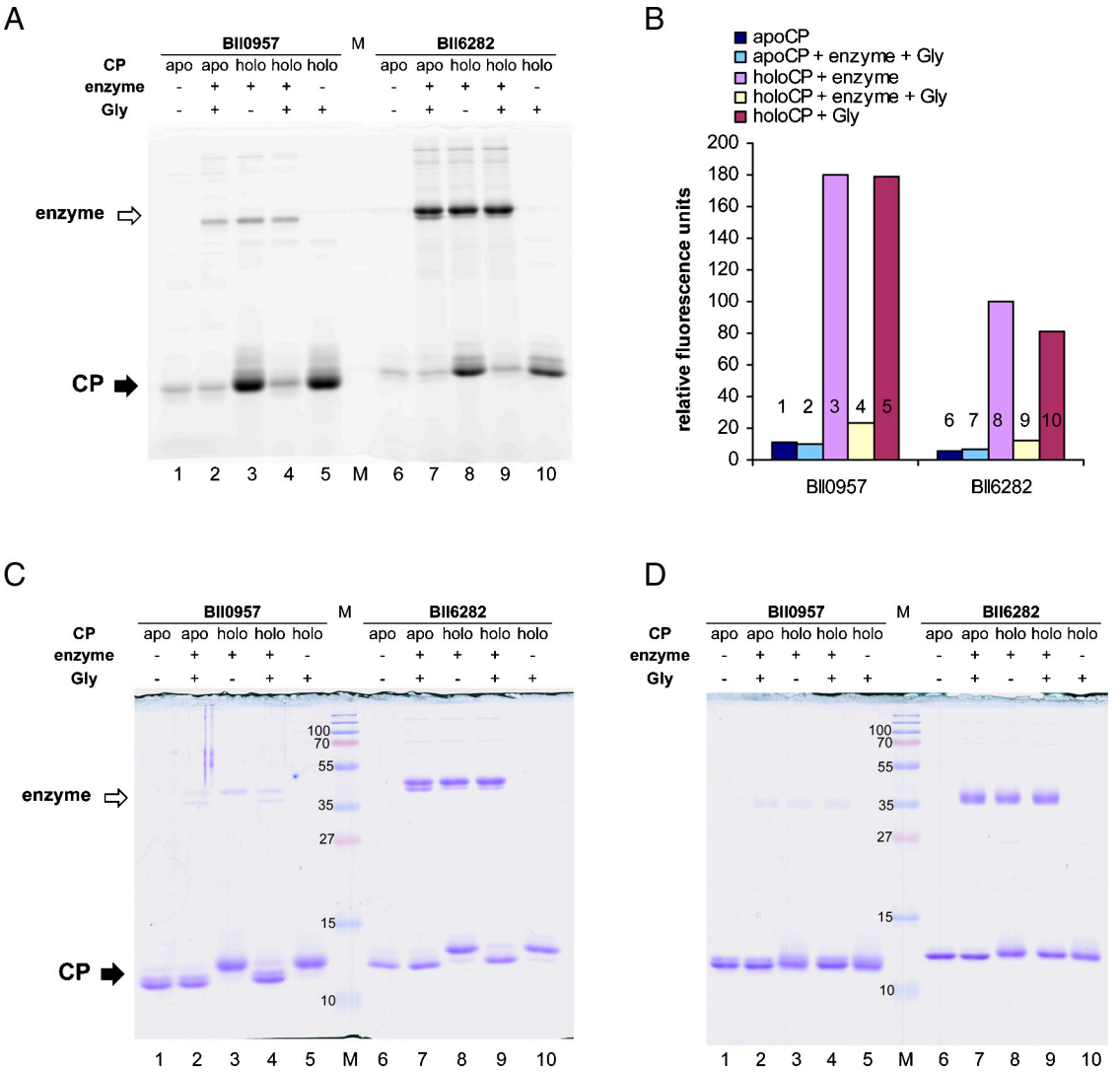

Fig. S5. Transfer of activated amino acids to cognate CPs by aSerRS homologs Bll0957 and Bll6282 CPs (1 μg/μL) were incubated with aSerRS homologs Bll0957 (0.1 μg/μL) or Bll6282 (0.8 μg/μL) in buffer containing 50 mM TrisHCl pH 7.5, 150 mM KCl, 10 % glycerol, 10 mM $MgCl_2$, 4 mM ATP, with or without 500 μM Gly for 45 min at room temperature. (*A*) Samples were treated with fluorescein-5-maleimide and subjected to SDS-PAGE. Fluorescently labeled proteins were detected using Typhoon Trio. (*B*) Densitometry of fluorescently labeled CP bands shown in *A*. After incubation with the enzymes and Gly, CPs were completely protected from fluorescent labeling (columns 4 and 9). (*C*) Gel shown in *A* after *Coomassie* staining. Binding of fluorescein affects electrophoretic mobility of CPs. CPs in the presence of the enzymes and Gly were completely protected from the labeling (lanes 4 and 9). (*D*) Control reactions untreated with fluorescein-5-maleimide. SDS-PAGE was conducted under nonreducing conditions, without addition of β-mercaptoethanol during sample preparation. Comparison of *A* and *B* to gel images *C* and *D* confirms that lower fluorescence intensity observed is not a consequence of -SH oxidation or CP degradation in the course of experiment. Differences in electrophoretic mobility in *C* and *D* (lanes 3, 5, 8, and 10) are caused by fluorescein binding to thiol group of phosphopantetheinylated CPs (holoCPs).

Table S1. Kinetic parameters for amino acid activation by aSerRS homologs determined in ATP-pyrophosphate exchange assay

		K_M, mM	k_{cat}, s^{-1}	k_{cat}/K_M, s^{-1} M^{-1}
Bll0957	Gly	0.93 ± 0.09	1.5 ± 0.1	1,680 ± 220
	Ala	25 ± 4	0.14 ± 0.02	5.4 ± 0.2
Bll6282	Gly	0.58 ± 0.03	1.01 ± 0.08	1,731 ± 73
	Ala	14 ± 2	0.075 ± 0.03	5.6 ± 0.4
Atu2573	Ala	0.24 ± 0.04	2.3 ± 0.3	10,200 ± 1,900
	Gly	5.7 ± 0.2	2.1 ± 0.1	373 ± 14
	Ser	5.6 ± 1.0	1.15 ± 0.05	234 ± 51
	Pro	46 ± 8	0.11 ± 0.01	2.4 ± 0.1
	Glu	54 ± 9	0.10 ± 0.01	2.0 ± 0.2

Values are given as arithmetic mean ± standard error of mean (SEM).

Table S2. Data collection and refinement statistics for Bll0957 structures

	Bll0957:AMP*	Bll0957:ATP*	Bll0957:GlyAMS*
Data collection			
Space group	$P2_12_12$	$P2_12_12$	$P2_12_12$
Cell dimensions			
a, *b*, *c* (Å)	127.7, 100.2, 50.2	127.2, 101.1, 50.4	128.1, 101.3, 50.5
α, β, γ (°)	90, 90, 90	90, 90, 90	90, 90, 90
	Peak		
Wavelength	1.28200	1.54056	1.54056
Resolution (Å)†	46.74 - 2.15 (2.28 - 2.15)	20.74 - 2.50 (2.64 - 2.50)	20.82 - 2.20 (2.32 - 2.20)
R_{sym} or R_{merge}†	0.098 (0.483)	0.130 (0.565)	0.120 (0.549)
$I/\sigma I$†	16.2 (3.4)	13.8 (3.2)	17.7 (4.5)
Completeness (%)†	99.4 (96.8)	99.8 (100.0)	99.6 (99.4)
Redundancy†	7.8 (7.2)	6.7 (5.7)	10.0 (10.1)
Refinement			
Resolution (Å)	29.78 - 2.15	20.74 - 2.50	20.41 - 2.20
No. reflections	35,847	23,162	33,974
R_{work}/R_{free}	0.1763/0.2084	0.1811/0.2315	0.1881/0.2276
No. atoms	4,911	4,760	4,890
Protein	4,681	4,532	4,545
Ligand/ion	58/2	62/4	54/2
Water	170	162	289
B-factors			
Protein	41.31	31.62	27.44
Ligand/ion	57.95/30.65	27.70/42.55	16.95/23.1
Water	43.72	29.43	32.00
rms deviations			
Bond lengths (Å)	0.010	0.010	0.009
Bond angles (°)	1.01	1.10	1.02

*One crystal was used for data measurement.

†Values in parentheses are for highest-resolution shell.